

Finite Element Analysis of Notch Depth and Angle in Notch Shear Cutting of Stainless-Steel Sheet

Kaan Emre Engin*

Adiyaman University, Faculty of Engineering, Turkey

Piercing is a crucial process in the sheet metal forming industry, and the surface quality of the pierced part is an important parameter that defines the overall quality of the product. However, obtaining a good surface quality is a challenging task that depends on the effect of several process parameters and necessitates the use of non-conventional procedures. Notch shear cutting is a relatively new progressive approach in which the workpiece is indented with a notch form with a predefined notch angle and depth, and then the indented workpiece is subjected to conventional piercing. In this study, conventional piercing and notch shear cutting processes were experimentally performed on 1.4301 stainless steel sheet of 2 mm thickness. Then, finite element (FE) analyses were conducted utilizing Deform-2D software. After ensuring that the experimental and simulation works were consistent with each other, the FE analysis of notch shear cutting was carried out for three distinct notch depths (15 %, 30 %, and 60 % of the workpiece thickness) and six different notch angles (10°, 20°, 30°, 40°, 50°, and 60°). Investigations were performed on shear zone length distributions, which are direct indications of the surface quality on sheared workpieces, crack propagation angles, and required cutting loads. The best surface quality was obtained when the notch angle was set to 50° and the notch depth was set to 15 % of the workpiece thickness. It was also observed that notch angle and notch depth had a certain level of influence on required cutting load.

Keywords: metal cutting, notch cutting, piercing, surface quality

Highlights

- The primary objective of the study was to determine the influence of notch angle and notch depth on surface quality and required cutting in notch shear cutting of 1.4301 sheets of 2 mm thickness.
- Both experimental and finite element (FE) analyses were performed to validate the consistency of two methods. Deform-2D software was utilized for numerical analysis whereas a die set was manufactured for experimental work.
- The overall best quality which surpassed the surface quality of piercing was achieved with a notch angle of 50° and a notch depth of 15 % of the workpiece thickness.
- It was determined that when the notch angle increased, the required cutting load decreased. This was also true for increasing notch depth, but the load incurred during the generation of notch depth must be included in the total energy consumption.

0 INTRODUCTION

Piercing is a fundamental process in the sheet metal forming industry and is defined as the cutting of the sheet metal from the stock with a die set consisting of a predefined shaped punch and a lower die. The primary purpose of the piercing process is to avoid workpiece rework and maintain good surface quality. Burrs and protruding surfaces create an impediment to achieving this goal. Burrs can cause early tool wear, reduced corrosion resistance and because of their sharp formations, can become the primary source of accidents. These negative impacts result in poor overall process production quality.

To remove these formations from the surface, conventional grinding and other cleaning procedures are necessary, resulting in additional labour hours, higher costs, and specific people being withdrawn from the main operating cycle and allocated solely to these deburring and cleaning activities [1].

Due to the nature of the process, numerous parameters should be adjusted and understanding the

effect of these parameters is the key step to achieving good cutting results and lower energy consumption. Adjustments in clearance [2] and [3], cutting speed [4], workpiece and tool material [5], tip form [6], tool coatings [7] and wear characteristics [8] to [12] have significant effects on both surface quality and energy aspects in conventional piercing procedures.

However, a relatively recent procedure known as “notch shear cutting” has been developed with the goal of improving the surface quality of sheared sheet components. A notch with specified characteristics is pushed onto the workpiece in this progressive method. The operation then proceeds with the conventional piercing method.

Few studies have investigated the notch shear cutting of sheets and related parameters. Studies investigating different aspects of the notch shear cutting proved that good surface quality with reduced burr formations can be achieved by using this method.

Sachnik et al. [13] used workpieces DC04, 1.4301, ENAW-6014 and CuSn6 with 1 mm thickness and performed both closed and open cuts with a

special progressive die. They mainly investigated the formation of burrs and how they change according to the notch placement on the workpiece. Both simulation and experimental works had been accomplished. The investigations were done for different values of notch cutting parameters as notch depth (30 % to 60 % of the sheet metal thickness), notch's radius (0.05 mm, 0.125 mm, and 0.2 mm) and clearance (6 %, 8 %, and 10 % of the material thickness). They showed that the burr formation is directly linked with the position of the notch and notch height. They also stated that around 40 % notch heights gave the most burr-free surfaces.

Krininger et al. [14] investigated the effect of notch parameters on the workpiece by using both experimental and finite element method (FEM) for sheet materials made of aluminium alloys ENAW-5754 and ENAW-6014 with a thickness of 1.0 mm. The clearance between the die and punch was 3 % of the workpiece thickness. They designed a progressive die set to perform the experimental work. Notches were both applied from the topsides and downsides of the workpiece; 25 % and 40 % of the notch depths and a fixed value of 60° as the notch angle were applied on the workpieces. They discovered that while the topside notch could lower the required cutting forces, in general, there was no reduction in cutting forces when the percentage drop in sheet thickness was considered. With downside notches, they observed that a surface distribution without burr could be achieved.

Feistle et al. [15] performed notch shear cutting studies on press-hardened components (PHC) made of aluminium-silicon-coated manganese-boron steel (22MnB5) sheets at room temperature. The shearing of PHC steels at room temperature causes difficulties due to their higher mechanical properties. Moreover, the wearing of tools progresses rapidly, which contributes to the formation of more burrs at the edges of the workpieces. The workpieces had 1.5 mm thickness. The die clearance was 15 % of the workpiece thickness. The notch angle was 60°. Notch depths were 16 % and 40 % of the workpiece thickness. Three notch variables (without notch, topside notch, and downside notch) were examined by both FEM and experimental methods. They measured the zone distributions on the sheared surfaces and calculated the required shearing force. They stated that cutting loads were reduced for notched specimens and provided improved surface quality free of burrs.

The existence of a notch on the workpiece introduces additional parameters to be investigated. The mentioned studies investigated some values of notch depth, but the notch angle values were generally limited to 60°. Furthermore, none of the

studies investigated the effect of these parameters on stainless steels which are one of the most used materials in industrial applications. The surface quality and required cutting load change according to notch depth and notch angle for stainless steels should be investigated with varied values of these two parameters. If correct parameter adjustments can be established for 1.4301 sheets during notch shear cutting and high surface quality can be produced, then a technical advantage can be acquired over conventional piercing techniques.

To achieve this, experimental and computational validations for conventional piercing and notch shear cutting were conducted initially. Following the consistency of the findings between experimental and computational work, three different notch depths (15 %, 30 % and 60 % of the workpiece thickness) and six different notch angles (10°, 20°, 30°, 40°, 50°, and 60°) were employed to execute the notch shear cutting of 1.4301 stainless steel sheet; the influence of these variables on the surface quality and required cutting load were investigated using finite element analysis.

1 PROCESS PARAMETERS

1.1 Notch Depth, Notch Angle, and Surface Distribution on the Workpiece

As an addition to the parameters of conventional piercing, notch shear cutting introduces new parameters such as notch depth, which is the percentage of the height of the notch to the thickness of the workpiece; notch angle, which is the angle value of the notch indented on the surface of the workpiece; and notch radius, which is the radius given to the tip of the notch.

Notch shear cutting is a progressive process. The related illustration of the steps of the process was given in Fig. 1. First, a notch indenter with a predetermined angle, depth, position, and radius is manufactured (Fig. 1a). In the second step, the indenter is forced against the workpiece, resulting in the development of a notch (Fig. 1b). Then, in the last step, the notched workpiece is subjected to conventional piercing and the process is completed (Fig. 1c).

Shearing of the material is a complicated phenomenon. When a workpiece is pierced, it goes through a series of stages before being entirely ruptured. Zones typical of piercing are generated on the workpiece's surface during these stages. Rollover (die roll) zone, shear (burnished) zone, fracture zone, and burr formation are the four zones mentioned. By measuring these zones and observing how much

they dominate the overall surface length, the surface quality of the sheared workpiece can be assessed.

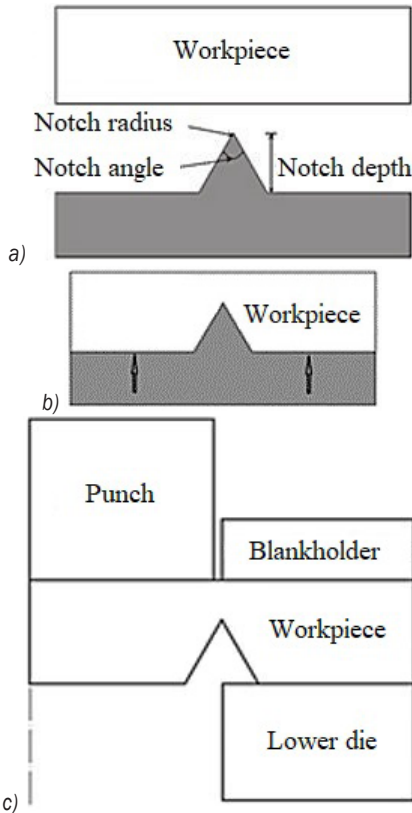


Fig. 1. The illustration of the steps of notch shear cutting and related components; a) manufactured indenter with predetermined notch properties, b) formation of notch on the workpiece and, c) conventional piercing of the notched workpiece

Rollover and burrs are the least desired zones on the surface, and investigations often involve methods and parameter modifications for eliminating these zones. Stahl et al. [16] implemented two-stage shear cutting instead of one-stage shear cutting of truck frame parts and revealed the effects of different process parameters on the improvement of surface quality and burr formations along with fatigue enhancement of the sheared parts. Mucha and Tutak [17] studied the impact of clearance on the burr size formed on a thin steel sheet with a 55 HRC hardness during the blanking of angled hooks, as well as the wear characteristics of the punch. Nishad et al. [18] collected and compared the methodologies used to improve the process and elaborated on how the parameters of the process impact the result. A long shear zone length is the most desired situation.

The illustration of these zones was given in Fig. 2. Denting the surface with a notch before piercing

has the potential to reduce burr forms while extending the shear zone length.

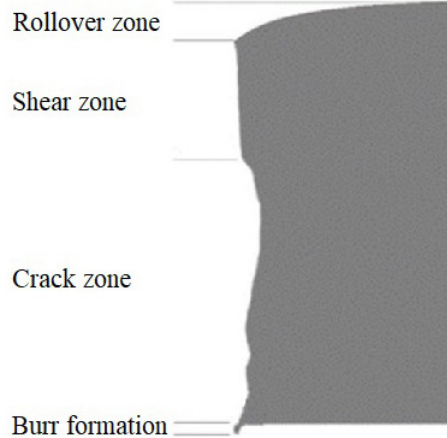


Fig. 2. Zone distributions on the sheared surface

Notch angle and depth are essential parameters that can influence crack propagation and orientation as well as zone distributions.

Determining the optimal values of these parameters are important. The upper limit of the notch angle value was set using a fine-blanking approach.

Generally, a notch is produced on the workpiece prior to cutting using a v-ring indenter to keep the workpiece in place and the side angle of the v-ring indenter is normally kept constant as 60° in related procedures like fine blanking. From this point of view, the upper limit of the notch angle was set at 60° ; moreover, 10° , 20° , 30° , 40° , and 50° were added to observe how they influenced the results. From low to high, notch depths were set at 15 %, 30 %, and 60 % of the workpiece thickness, respectively.

2 EXPERIMENTAL METHODOLOGY

The first step in the study was to conduct the experiments. Although this study relied heavily on finite element (FE) analysis, computational results should be cross-checked with experimental data. If computational and experimental work for piercing and notch shear cutting could be verified to be consistent with one another, the simulation work would be expanded to study the influence of other notch shear cutting parameters.

The stock material was 1.4301 stainless steel sheet. The mechanical characteristics of the material have crucial importance in shear-cutting processes. Due to this situation, the mechanical characteristics of 1.4301 sheet were determined as the beginning phase of the research. If the mechanical characteristics

of the workpiece material were defined with errors in the software, the results would almost certainly differ from those obtained via experimental work. 1.4301 stainless steel sheet is used in a variety of industrial applications, including mining, maritime and structural applications as well as the manufacture of bolts, screws, and containers [19].

Tensile tests were used to get the stress-strain graphs that the software required. A stock 1.4301 stainless steel sheet was supplied from local sheet metal vendors. The dimensions of the stock material were 2000 mm × 1000 mm with 2 mm thickness to satisfy the tensile testing standards. The chemical composition and the mechanical properties of the material according to the manufacturer’s sheets are given in Tables 1 and 2.

Table 1. Chemical composition of 1.4301 sheet

Composition	Weight [%]	Composition	Weight [%]
C	0.08	Si	0.75
Mn	2.0	S	0.03
P	0.04	Ni	9.0
Cr	19.0		

Table 2. Mechanical Properties of 1.4301 sheet

Properties	Value	Properties	Value
Tensile strength	515 MPa	Elongation at break	60 %
Yield strength	210 MPa	Hardness (Rockwell B)	80

Using a water jet, the specimens were cut out of the stock according to ASTM E8 standards, considering the rolling directions (0°, 45°, 90°). The goal of using a water jet is to lessen the thermal effects that arise on the material’s surface. The sides of the specimens were also polished to prevent the notch effect from occurring during tensile tests. Fig. 3 shows the dimensions of the test specimen (Fig. 3a) and the actual test specimen (Fig. 3b).

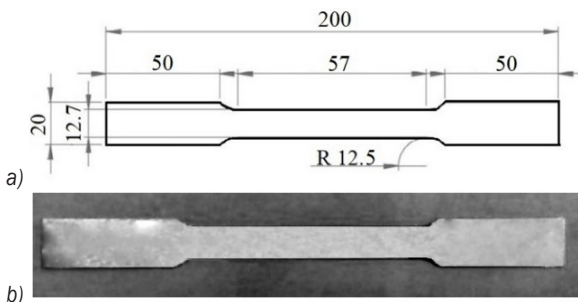


Fig. 3. a) Dimensions, and b) the actual image of one of the tensile test specimens

Fig. 4 depicts the metallographic structure of 1.4301 sheet observed by using a scanning electron microscope (Zeiss Gemini SEM 500). A Shimadzu AG-X Plus tensile testing machine was used to measure the engineering curve of 1.4301 sheet.

To reduce the margin of error, the tensile tests were repeated six times at room temperature for each rolling direction at a strain rate of 0.05 s⁻¹.

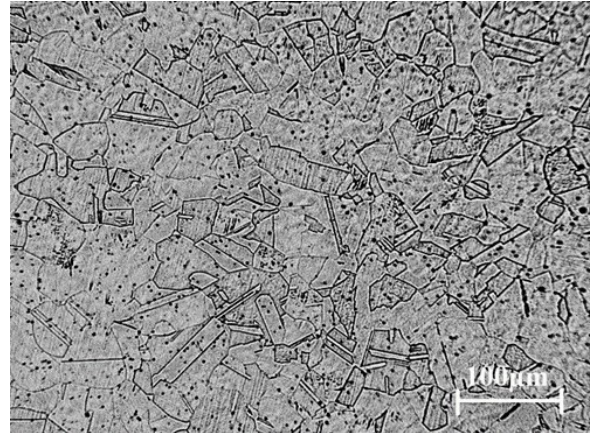


Fig. 4. Metallographic structure of 1.4301 stainless steel sheet

First, engineering stress was measured, and then true stress is obtained by using true stress-strain equations expressed in Eqs. (1) and (2) as:

$$\sigma_t = \sigma(1 + \epsilon), \tag{1}$$

$$\epsilon_t = \ln(1 + \epsilon), \tag{2}$$

where σ_t and σ represent true and engineering stresses, ϵ_t and ϵ are true and engineering strains. The obtained engineering and true stress-strain curve of 1.4301 sheet were given in Fig. 5.

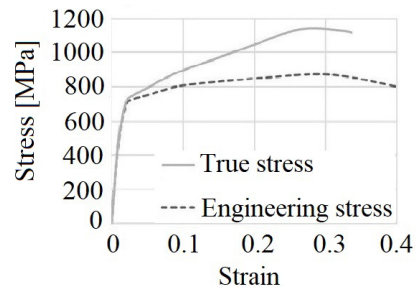


Fig. 5. True and engineering stress-strain diagram of 1.4301 stainless steel sheet

In the second phase, both piercing and notch shear-cutting operations were carried out experimentally. A manufactured die set was used to perform piercing and notch shear cutting. It consisted of six parts: the

punch, upper die block, guides, a fixed-type blank holder, lower die, and lower die block. The blank holder and die blocks were constructed of S235JR, while the remainder of the components were made of heat-treated 1.7225 steel. The die set (Fig. 6a) and its exploded view (Fig. 6b) are shown.

Due to the progressive nature of notch shear cutting, which necessitates the formation of a notch on the workpiece's surface before conventional piercing can begin, a special hollow punch was produced to be used as an indenter. The manufactured hollow punch's tip sides had a 60° notch angle and a notch tip radius of 0.5 mm. The depth of the hollow was adjusted to 1.2±0.1 mm to prevent the hollow punch to penetrate further than the notch depth of 60% of the workpiece thickness. The total length of the punch was 80 mm. Fig.7 shows the illustration of the hollow punch (Fig. 7a) and the formation of the notch indenter (Fig. 7b).

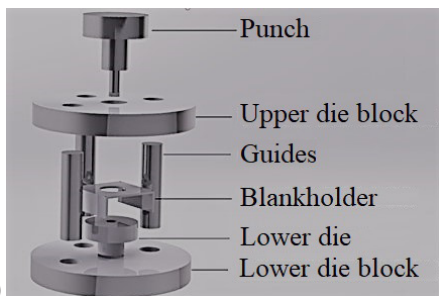
Clearance between the die and the punch was calculated according to Eq. (3) as:

$$C = 100((D_m - D_p)/2t) [\%], \quad (3)$$

where D_m is the lower die diameter, D_p is the punch diameter and t is the workpiece thickness.



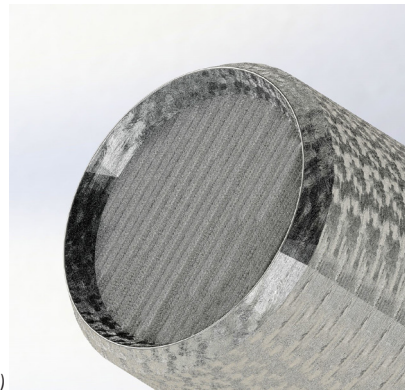
a)



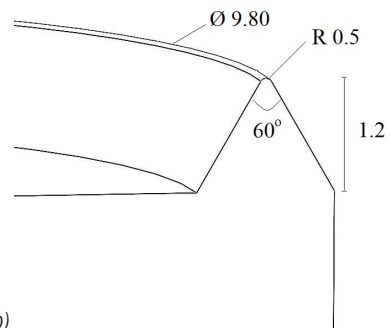
b)

Fig. 6. a) The die set, and b) it's exploded view

The die clearance was fixed at 5 % of the thickness of 1.4301 sheet, which was 2 mm, for both experimental and computational work.



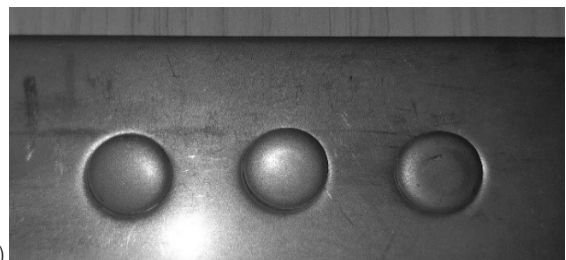
a)



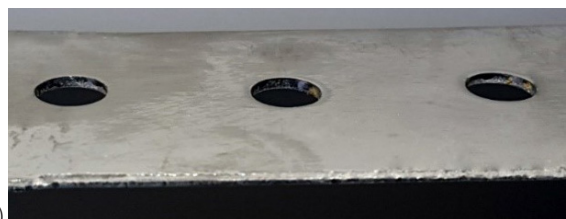
b)

Fig. 7. a) Illustration and b) dimensions of hollow punch in [mm]

The lower die diameter was 10 mm; based on Eq. (3), the calculated and fabricated punch diameter to perform a conventional piercing process was 9.80 mm. The total length of the punch was 80 mm. Experiments were conducted utilizing a hydraulic press with a capacity of 300 kN and under a ram speed of 1 mm/s. To keep the punches in place, a punch holder was manufactured and attached to the press's ram.



a)



b)

Fig. 8. a) Notch indentations on the workpiece, and b) conventionally pierced workpiece

The piercing operation was carried out using the manufactured die set while the notch shear-cutting process was carried out in a progressive manner. The notch is first produced on the downside of the workpiece. Following that, the standard piercing process was performed. Fig. 8 shows an example of notch creation on the workpiece surface (Fig. 8a) and one of the typically pierced workpieces (Fig. 8b), respectively.

3 NUMERICAL SIMULATION AND MODEL VERIFICATION

Deform-2D software was used to execute the computational work. Sheet metal shearing is one of the many forming techniques that the software can model. The software employs axisymmetric modelling which implies that only half of the setup is required to run it. The workpiece was modelled as a plastic object, whereas the punch, lower die and blank holder were defined as rigid bodies. Shear friction occurs when the workpiece deforms and is a function of the yield stress. The friction between the workpiece and the shearing tools was assumed to remain constant and was calculated as follows in Eq. (4):

$$f_s = mk, \tag{4}$$

where f_s is the frictional stress, k the shear yield stress, and m the friction factor. According to the software's database, shear friction was given a value of 0.12.

Large plastic stresses are generated over a narrow zone between the punch and the die during shearing. At that small deformation zone, the material was considered to be isotropic and yielding followed Holloman's equation which was stated in Eq. (5) as:

$$\bar{\sigma} = K\varepsilon^{-n}, \tag{5}$$

where $\bar{\sigma}$ is the effective stress, ε the effective strain, K is the material constant, and n the strain hardening exponent [20].

Deform-2D database includes the material properties for 1.4301 stainless steel. Fig. 9 demonstrated the consistency of the flow stress-strain curve of 1.4301 stainless steel in Deform-2D's database and the computed flow stress-strain curve obtained from the tensile tests by using Holloman's equation.

Fracture initiation in a piercing process usually begins at the punch's or lower die's contacting edge. For computational studies, the fraction criterion is critical because good criterion choice brings the outcome values closer to the experimental results.

For the purposes of numerical analyses, the normalized Cockroft and Latham fracture criterion were utilized.

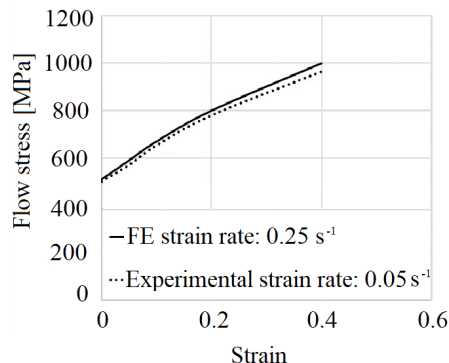


Fig. 9. Flow stress-strain curve of 1.4301 stainless steel

The criterion indicates that when effective strain equals the critical value (C), fracture initiation begins at the point where the value is reached. The criterion was given in Eq. (6) as:

$$\int_0^{\varepsilon^f} \left(\frac{\sigma^*}{\bar{\sigma}} \right) d\bar{\varepsilon} = C, \tag{6}$$

where σ^* is the maximum principal stress, ε^f the fracture strain, C the critical value (damage factor), and $\bar{\sigma}$ and $\bar{\varepsilon}$ are the expressions of effective stress and effective strain.

To simplify the criterion, the ratio between maximum principal and effective stress was assumed to be constant at the shearing zone. This assumption resulted in $\varepsilon^f = C$ meaning that crack initiation starts at the point where effective strain and critical values become equal [21].

The critical value, C , can be evaluated by a tensile test regardless of the working operation. The critical value of 1.4301 sheet was defined as 0.54, which was acquired from the conducted tensile test.

The software employs a step-based iteration mechanism; at each step, it verifies the workpiece's values. If the values described by mesh formations on the workpiece approach the critical value, element deletion is applied to the associated meshes to view the fracture initiation and propagation. This function is governed by two parameters: "fracture steps" and "fracture elements." The value of fracture steps sets the step interval at which the simulation pauses and element deletion is performed. This value was selected as 1, the minimal value. This signifies that element deformation is considered at each step. Fracture elements are the number of elements that must exceed

the critical damage value for the simulation to halt and delete elements. This value was set as the system default to 4. Automated mesh generation was used and defined to be executed for every 0.02 mm progression of the top die to provide optimum re-meshing.

Element deletion improves visualization coherence with experimental outcomes. However, negative aspects of this approach include volume deterioration and excessive mesh deletion if mesh element numbers are maintained low. Low mesh numbers result in an imprecise representation of the shear region where the zones interweave. This circumstance results in inaccurate calculations of the cutting load and interpretations of the zone lengths derived from simulation results.

The density of the meshes at the shear zone must be as dense, small, and numerous as possible to prevent volume loss and accurate propagation of the fracture, which enables consistent visualization of the variation in zone distribution. Initially, the meshes on the workpiece were evaluated with varying element counts; however, as the element count reached 8,100, isoparametric quadratic elements, it was determined that there was no change in cutting load above this element count. Tough, to obtain optimum surface distribution on the sheared workpieces, 10,000 isoparametric quadratic elements which are the maximum number of elements that can be defined in Deform-2D and 9,786 number of nodes with 0.03 mm element size were used. The simulation parameters were given in Table 3.

Table 3. Simulation parameters

Parameter	Value
No. of elements	10,000
No. of Nodes	9,786
Element size	0.03 mm
Fracture steps	1
No. of fracture elements	4
Remesh criteria	Every 0.02 mm of the punch penetration

In addition, mesh elements were stacked as closely as possible with the use of mesh windows to raise the total number of elements in the shearing zone.

For both piercing and notch shear cutting processes, the distribution of zones and the cutting load values were estimated after conducting both computational and experimental work.

The numerical analysis phase of the notch shear-cutting process required two sequential steps to duplicate experimental conditions for the most

accurate results. Fig. 10 shows the steps applied during the computational work of notch shear cutting. First, it was necessary to push the predefined notch indenter into the workpiece (Fig. 10a) and produce the indentation (Fig. 10b). The notched workpiece was then placed in a typical piercing setup (Fig. 10c) and the following steps were carried out (Fig. 10d).

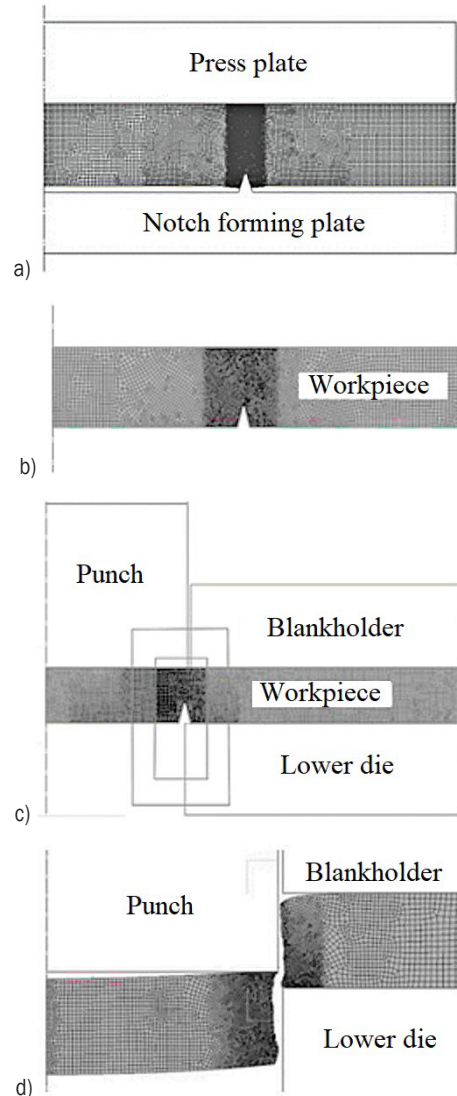


Fig. 10. The steps of simulation process; a) formation of notch at the downside of the workpiece, b) notched workpiece, c) conventional piercing, and d) completion of the process

3.1 Ideal Crack Condition

During a shearing operation, the fracture of the material begins at the corners of the punch and die that are in contact. The creation of a fracture propagates rapidly, resulting in the separation of

material at the intersection with the opposite corner. The ideal crack (Φ) occurs when the required angle of crack propagation (θ) is directed toward the punch and die cutting edges. In many instances, however, the real propagation (β) of a fracture does not follow this anticipated pattern, resulting in secondary cracks that cause surface flaws on the workpiece. When the angle values of β and θ are closest, the optimal cutting condition may be attained.

This situation can be expressed in Eq. (7) as:

$$\Phi = \beta - \theta \cong 0 . \tag{7}$$

The ideal crack propagation angle can be expressed in Eq. (8) as:

$$\theta = \text{Arctan} \left(\frac{c}{t - u_p} \right), \tag{8}$$

where C is the clearance, t the sheet metal (workpiece) thickness, and u_p the punch penetration corresponding to the first crack initiation within the sheet. The directions of angle β and angle θ were illustrated in Fig. 11.

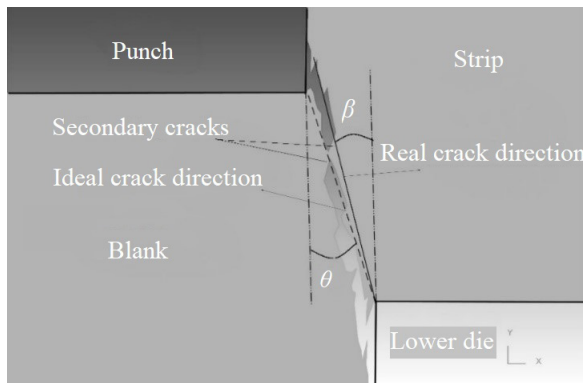


Fig. 11. Illustration of Ideal crack propagation angle (θ) and real crack propagation angle (β)

4 RESULTS AND DISCUSSION

Both experimental and numerical work were performed under the clearance value of 5 % of the workpiece thickness which was 2 mm, with a 10 mm lower die diameter and 9.80 mm punch diameter for conventional piercing with a punch speed of 1 mm/s.

Throughout the notch formation sequence, the hollow punch with a 60° notch angle, a notch tip radius of 0.5 mm, and a notch depth of 60 % of the workpiece thickness (1.2 ± 0.1 mm) was utilized. During the second phase (piercing after notch generation) of notch shear cutting, the same settings as with conventional piercing were employed.

Fig. 12 depicts a comparison of the change in cutting load between simulation and experimental tests.

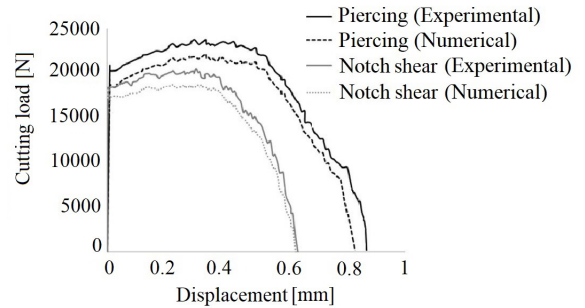


Fig. 12. Comparison of required cutting load between computational and experimental work

The experimental and numerical findings were within 5 % range of each other on average. This was the outcome of the experimental environment’s external influences such as dust, additional friction between tools and load cell accuracy. The rest of the research was carried out with computational work once the measurements were verified to be identical.

Figs. 13 and 14 compare the zone distribution for conventional piercing and notch shear cutting, respectively.

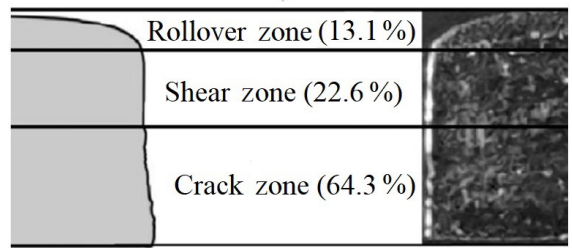


Fig. 13. Comparison of zone distributions between computational and experimental work (Piercing)

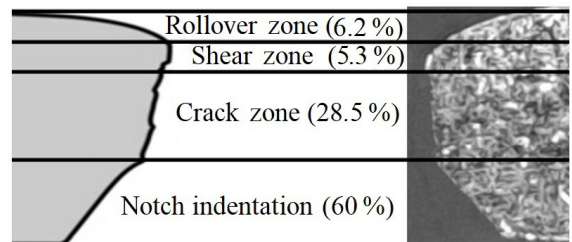


Fig. 14. Comparison of zone distributions between computational and experimental work (Notch shear cutting)

The computational work was completed by following the outlined sequential stages to replicate the experimental work. First, three values of notch depth

(15 %, 30 % and 60 % of the material thickness) and 6 different notch angles (10°, 20°, 30°, 40°, 50°, and 60°) with 0.5 mm notch tips were virtually penetrated to the downside of 1.4301 sheet with 2 mm thickness. After the material was notched, the piercing stage of the process was simulated using the configuration in which the lower die diameter was 10 mm, the punch speed was 1 mm/s, and the clearance was 5 % of the material thickness. As in the experimental study, the punch diameter was 9.80 mm, no radiuses were specified at the punch's edges, and the tip of the notch was aligned with the punch's cutting edge at shearing in every simulation.

Required cutting loads to shear the workpiece, fracture propagation angles and zone distributions were investigated. In cutting operations, cutting load is an important parameter that specifies the required loading capacity of the press and plays a crucial role in overall energy usage. It was discovered that the cutting loads necessary to shear notched materials were less than the load value for the piercing operation (28.5 kN). The deeper the notch penetrated into the material; the less cutting force was required at the sequential piercing step. This outcome was anticipated due to the reduction in material thickness following the creation of a notch in the workpiece. A 15 % notch depth resulted in the highest whereas 60 % notch depth resulted in the lowest required cutting load for each notch angle. For example, when the notch angle was fixed to 60°, the required cutting loads were obtained 22.2 kN for 15 % notch depth, 16.6 kN for 30 % notch depth, 11.8 kN for 60 % notch depth, respectively. The effect of the notch depth on the required cutting load is unique to notch shear cutting, regardless of the workpiece shape, and is consistent with the literature [22]. Another observation was made on the effect of notch angles. Apart from the notch depth, the required cutting load decreases with increasing notch angle due to the decrease in the cross-sectional area of the workpiece between the punch and die. The changes in required cutting load according to notch depths and angles are given in Fig. 15.

Although it might be thought that a deeper notch has the advantage of a lower cutting load, it is important to remember that two phases are necessary to complete the entire notch shear-cutting process. If load comparisons were conducted exclusively for the shearing portion of the operation, it might be argued that a notch could reduce the cutting load.

To account for each phase of the operation, however, 15 kN should be added to the total load values which was the average of the loads required

to form the notch into the surface of 1.4301 sheet for each of the depths listed.

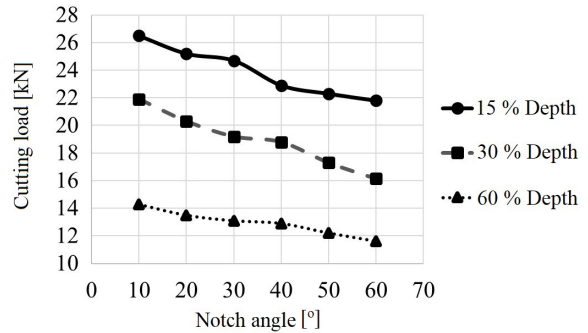


Fig. 15. Cutting load change according to notch angle and notch depth

Fig. 16 illustrated the disparities between the ideal angle (θ) of crack propagation and the real angle (β) of crack propagation.

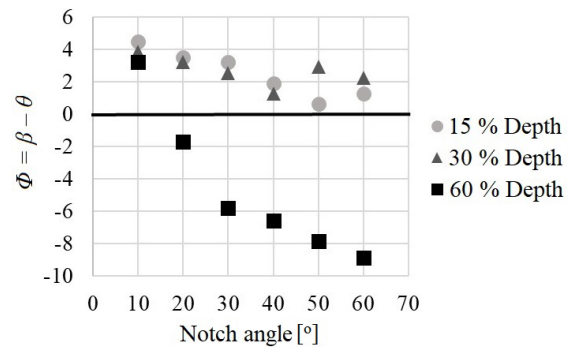


Fig. 16. The difference between real crack propagation angle (β) and ideal crack propagation angle (θ)

The best surface quality can be achieved when the difference between these two angles is closest to zero.

The distribution of zones and the propagation of cracks are interrelated; therefore, an improper crack propagation difference will lead to secondary cracks and protruding surfaces.

Deform-2D can measure distances on the sheared workpiece in relation to zone distributions, and the character of the cut (smooth or protruded) can be clearly visualized and estimated by using the software's post-processor section once the simulation is complete. Fig. 17 shows the shear zone percentage change according to notch depth and notch angle.

A comparison of Figs. 15 and 16 demonstrated that the difference between crack propagation angles and shear zone percentages were in correlation. For piercing processes, the optimal zone distribution

(best surface quality) occurs when the rollover and crack zone lengths are minimal and free of burr formation while the shear zone length is maximal; 15 % of the notch depth with 10°, 20°, and 30° notch angles resulted in burr formation, which was the least desirable outcome. The development of protrusions reduced as the notch angle increased, and at 50° the longest shear zone length and the shortest crack zone with almost no protrusions were reached.

From Fig. 16, it was observed that the closest values to zero amongst all notch depths and all notch angles were achieved when notch angle value was selected as 50° and the notch depth value was selected as 15 % of the workpiece thickness. Fig. 17 confirmed this result, the shear zone percentage, 24.56 %, was also the highest at these values.

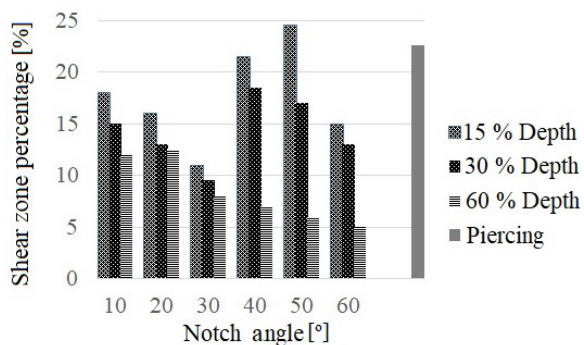


Fig. 17. Shear zone percentage change according to notch depth and notch angle

The shear zone length of the specimen measured after piercing (22.6 %) could only be surpassed by using these values. This situation showed that a technical advantage can be obtained over conventional piercing with proper adjustments. The relationship between crack propagation angles and shear zone percentages was in accordance with previous studies. Using the angles of crack propagation, Hambli et al. [23] devised an algorithm for predicting optimal clearance. They established a tolerance convergence percentage of 1 % and stated that an optimal clearance could be reached when the difference between crack angles satisfied this value, indicating that no secondary cracks occurred, and good surface quality was acquired. Engin and Eyercioglu [24] and [25] studied the influence of different process parameters on 1.4301 stainless steel sheets with different thicknesses and diameters. They observed that the best surface quality on the sheared workpieces was achieved when the difference between crack propagation angles was minimal. Fig. 18 displays the surfaces of sheared workpieces in relation to the notch depth, notch angle,

and independently for piercing, as established by the Deform-2D software.

A further observation was made on another impact of notch depth. It was determined that the length of the shear zone dropped dramatically when the notch depth increased, independent of the notch angle. This is due to the workpiece's pre-deformation during notch formation.

When the workpiece was subjected to the conventional piercing phase, which was the second step of the process, shear and fracture zones were generated following the top portion of the notch.

In the case of deeper notches, there remained a reduced region for shear zones to develop, and this was the main reason for the drop in shear zone length. Figs. 17 and 18 demonstrated that the crack zone dominated the surface and the shear zone decreased below 7 % for notch angles between 40° and 60° and for 60 % notch depth. This case revealed that even though pre-deformation (notch) on the workpiece appeared to make the shearing region less affected during piercing, deeper notches were not a guarantee of high surface quality and notch angles should be taken into consideration.

Regardless of notch depth, notch angles determined the crack propagation course and, in turn, affected the shear zone length. It was clearly understood that the obtained results depended on the combined effect of notch angle and notch depth values. For every notch depth value, the notch angle difference altered the crack propagation. As indicated before, for 15 % notch depth, lower notch angle values resulted in burr formation. When notch angle values increased, burr formations started to reduce up to a limit where the best surface quality could be obtained. In the event of higher notch depths, such as 30 %, the shear zone lengths decreased incrementally from 15 % to 10 % between 10° and 30° notch angles but reached their peak at a 40° notch angle with a length value of 22.43 %, and then started to decrease again.

This situation showed that for every value of notch depth, there exists a notch value at which the shear zone length could reach its peak height.

This criterion was met with a 50° notch angle at 15 % notch depth, a 40° notch angle at a 30 % notch depth, a 20° notch angle at a 60 % notch depth for 1.4301 sheet, respectively.

However, it should be clearly stated that the general form of the sheared surfaces is also an important parameter. As mentioned before, the primary objective was to obtain the best possible surface quality to transcend conventional piercing. For deeper penetrations such as 30 % and particularly

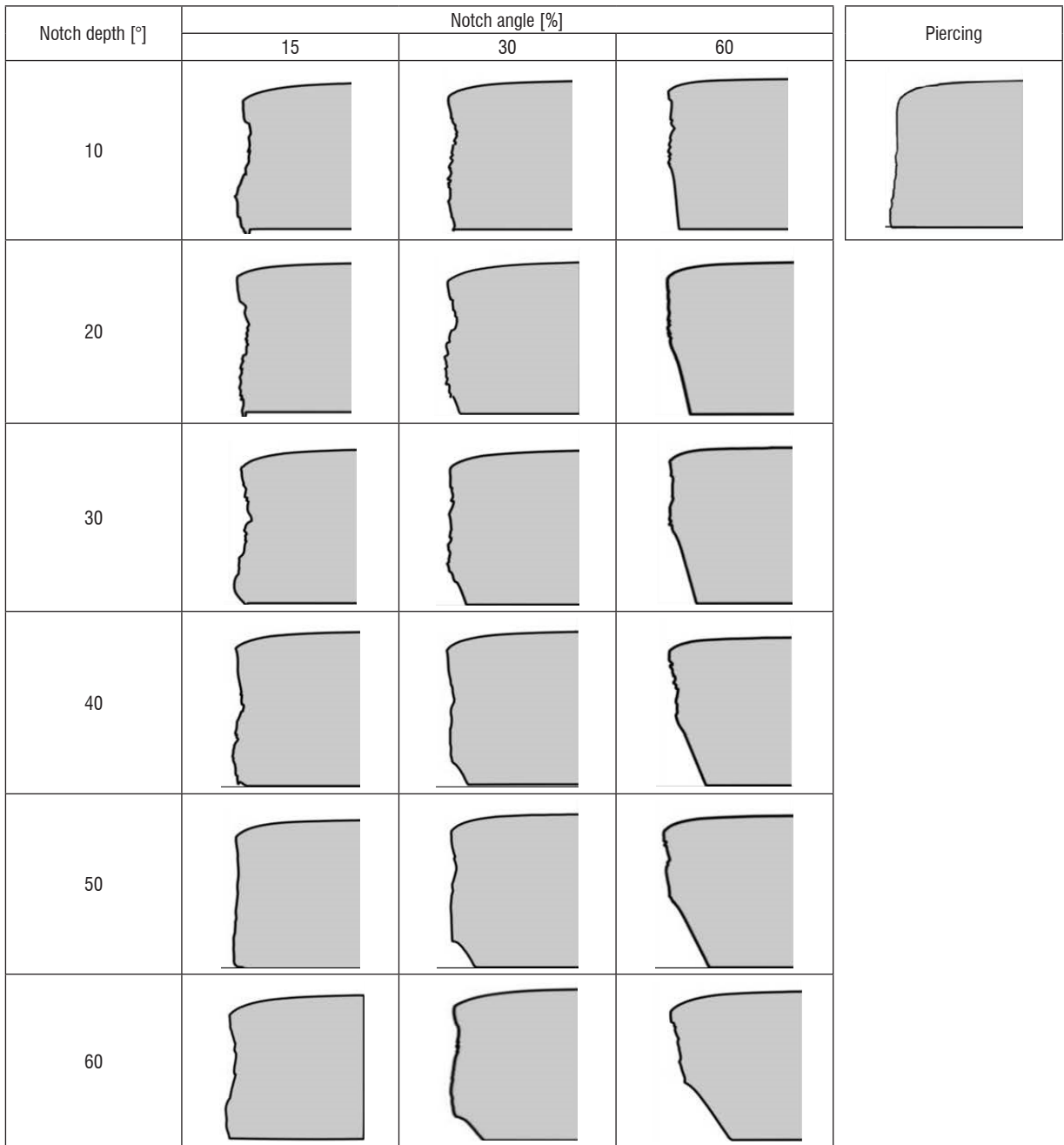


Fig. 18. Visual representation of sheared parts as a function of notch depth and notch angle generated by the Deform-2D software

60 % notch depths, the increase in the notch angle resulted in the reduction of burr formation; however, the form of the workpiece gradually deteriorated and took a conical shape at the downside. This circumstance is equally undesirable. At high values of notch depth, it must be considered that the use of wider notch angles may result in the deformation of the sheared material's shape.

Typically, the outputs of piercing/ shearing processes are restricted to the parameters applied specifically for that workpiece material. The same situation applies to this research. In terms of zone distributions, a 50° notch angle and 15 % notch depth outperformed the shear zone length value of conventional piercing to produce the greatest surface quality and form. However, it is limited to

1.4301 sheets if and only if these conditions are satisfied. Any change in the notch forming position, clearance, punch/die diameters, shearing speed and, most importantly, the workpiece material modifies every effect and may result in varied outputs. Due to the interdependent interactions between regulating parameters, it is difficult to establish an optimal setting for shearing and cutting operations that accounts for all process variables and workpiece materials.

5 CONCLUSIONS

The main aim of this study was to determine the effect of notch angle and notch depth on the surface distribution and required cutting force during notch shear cutting of 1.4301 stainless steel sheet workpieces to fill a gap in the literature due to an absence of research on notch shear cutting of commonly used stainless steels. Compared to piercing, notched shear cutting is a relatively novel method for cutting metal sheets. Conventional piercing and notch shear cutting were carried out to compare the results to those obtained from simulations. The remainder of the study is then completed virtually. Using Deform-2D software, a FEM study of notch shear cutting was performed for three different notch depths (15 %, 30 %, and 60 % of the workpiece thickness) and six different notch angles (10°, 20°, 30°, 40°, 50°, and 60°). The results obtained in this study are summarized below.

- For specimens with deeper notches and wider notch angles, the required cutting load was observed to decrease. In addition, cutting specimens with notches required less load than conventional piercing. This is a direct by-product of the material's decreased thickness due to the notch formation on the workpiece. Due to the progressive nature of the operation, the load applied during notch formation must be added to the total value of the required cutting load, resulting in an increase in total energy consumption. In addition, it may take longer to complete the whole process than piercing, which is not a progressive operation like notch shear cutting.
- There was an ideal value for each notch depth and notch angle at which the sheared surface was as good as possible in comparison to the other values for these two parameters. This condition was achieved at a 50° notch angle for a 15 % notch depth, at a 40° notch angle for a 30 % notch depth, and at a 20° notch depth for 60 % notch angles, respectively. In contrast to the

ideal values, however, values that depart from them might lead to increased surface flaws. In addition, the specimen's base became conical due to the increasing notch depths and notch angles (such as 60 % notch depth and 60° notch angle) which is undesirable. The shear zone length of the specimen estimated after piercing (22.6 %) could only be exceeded by notch shear cutting with a 50° notch angle and 15% notch depth (24.4 %). The remaining shear zone values were inadequate for shearing 1.4301 sheets when compared to conventional piercing.

- If surface quality is of the highest significance and no rework of the produced workpieces is necessary during the production, notch shear cutting can produce better results than piercing, particularly in preventing burr forms. However, to attain the maximum shear zone length with no burrs, preliminary work should be conducted prior to application, since any uncorrected value may cause the shear zone to be shorter than piercing. Hence, obtaining the optimal settings is a complex and expensive operation to be accomplished through experimental trial and error, FEM simulations are required to conduct the work. Nonetheless, it is a time-consuming endeavour. Notch shear cutting seems feasible when utilized for mass manufacturing.
- All findings are explicitly limited to the shearing of 1.4301 stainless steel sheets and under the specified parameters. Any change in the material properties or unstudied aspects, such as notch position, various clearance values and cutting speed, might substantially vary the obtained results.

6 REFERENCES

- [1] Gomah, M., Demiral, M. (2020). An experimental and numerical investigation of an improved shearing process with different punch characteristics. *Strojniški vestnik - Journal of Mechanical Engineering*, vol. 66, no. 6, p. 375-384, DOI:10.5545/sv-jme.2020.6583.
- [2] Li, X. Chen, Z. Dong, C. (2021). Failure and forming quality study of metallic foil blanking with different punch die clearances. *International Journal Advanced Manufacturing Technologies*, vol. 115, p. 3163-3176, DOI:10.1007/s00170-021-07400-z.
- [3] Lo, S.-P., Chang, D.-Y., Lin, Y.-Y. (2007). Quality prediction model of the sheet blanking process for thin phosphorous bronze. *Journal of Materials Processing Technology*, vol. 194, no. 1-3, p. 126-133, DOI:10.1016/j.jmatprotec.2007.04.110.
- [4] Liewald, M., Bergs, T., Groche, P., Behrens, B.A., Briesenick, B., Müller M., Niemiets P., Kubik, C., Müller, F. (2022).

- Perspectives on data-driven models and its potentials in metal forming and blanking technologies. *Production Engineering*, vol. 16, no. 5, p. 607-625, DOI:10.1007/s11740-022-01115-0.
- [5] Lubis, D.Z., Indrasepta, L.R., Bintara, R.D., Ramadhan, R., Darmawan, A.B. (2021). The effect of thickness and type of material on the sheared edge characteristics of keychain cranioplasty plate blanking product using eccentric press machine. *Journal of Mechanical Science and Technology*, vol. 5, no. 1, p. 29-35, DOI:10.17977/um016v5i12021p029.
- [6] Mori, K., Abe, Y., Kidoma, Y., Kadarno, P. (2013). Slight clearance punching of ultra-high strength steel sheets using punch having small round edge. *International Journal of Machine Tools and Manufacture*, vol. 65, p. 41-46, DOI:10.1016/j.ijmachtools.2012.09.005.
- [7] Klocke, F., Sweeney, K., Raedt, H.-W. (2001). Improved tool design for fine blanking through the application of numerical modeling techniques. *Journal of Materials Processing Technology*, vol. 115, no. 1, p. 70-75, DOI:10.1016/S0924-0136(01)00771-3.
- [8] Guo, W., Tam, H.-Y. (2012). Effects of extended punching on wear of the WC/Co micropunch and the punched microholes. *The International Journal of Advanced Manufacturing Technology*, vol. 59, p. 955-960, DOI:10.1007/s00170-011-3567-0.
- [9] Ko, D.-C., Kim, D.-H., Kim, B.-M. (2002). Finite element analysis for the wear of Ti-N coated punch in the piercing process. *Wear*, vol. 252, p. 859-869, DOI:10.1016/S0043-1648(02)00032-7.
- [10] Mucha, J. (2010). An experimental analysis of effects of various material tools wear on burr during generator sheets blanking. *International Journal of Advanced Manufacturing Technology*, vol. 50, p. 495-507, DOI:10.1007/s00170-010-2554-1.
- [11] Mucha, J., Jaworski, J. (2016). The tool surface wear during the silicon steel sheets blanking process. *Maintenance and Reliability*, vol. 18, no. 3, p. 332-342, DOI:10.17531/ein.2016.3.3.
- [12] Mucha, J., Jaworski, J. (2017). The Quality Issue of the parts blanked from thin silicon sheets. *Journal of Materials Engineering and Performance*, vol. 26, p. 1865-1877, DOI:10.1007/s11665-017-2589-7.
- [13] Sachnik, P., Hoque, S.E., Volk, W. (2017). Burr-free cutting edges by notch-shear cutting. *Journal of Materials Processing Technology*, vol. 249, p. 229-245, DOI:10.1016/j.jmatprotec.2017.06.003.
- [14] Kringinger, M., Feistle, M., Golle, R., Volk, W. (2017). Notch shear cutting of aluminum alloys. *Procedia Engineering*, vol. 183, p. 53-58, DOI:10.1016/j.proeng.2017.04.010.
- [15] Feistle, M., Kringinger, M., Golle, R., Volk, W. (2012). Notch shear cutting of press hardened steels. Merklein, M., Duffou, J. R., Leacock, A. G., Micari, F. Hagenah, H. (Eds.), *Key Engineering Materials*. Trans Tech Publications Ltd, Pfaffikon, p. 477-484, DOI:10.4028/www.scientific.net/KEM.639.477.
- [16] Stahl, J., Pätzold, I., Golle, R., Sunderkötter, C., Sieurin, H., Volk, W. (2020). Effect of one-and two-stage shear cutting on the fatigue strength of truck frame parts. *Journal of Manufacturing and Materials Processing*, vol. 4, no.2, p. 52, DOI:10.3390/jmmp 4020052.
- [17] Mucha, J., Tutak, J. (2019). Analysis of the influence of blanking clearance on the wear of the punch, the change of the burr size and the geometry of the hook blanked in the hardened steel sheet. *Materials*, vol. 12, no. 8, art. ID 1261, DOI:10.3390/ma12081261.
- [18] Nishad, R., Totre, A., Bodke, S., Chauhan, A. (2013). An overview of the methodologies used in the optimization processes in sheet metal blanking. *International Journal of Mechanical Engineering and Robotics Research*, vol. 2, no. 2, p. 307-318.
- [19] Kumar, A., Sharma, R., Kumar, S., Verma, P. (2022). Review on machining performance of AISI 304 steel. *Materials Today: Proceedings*, vol. 56, p. 2945-2951, DOI:10.1016/j.matpr.2021.11.003.
- [20] Sahli, M., Roizard, X., Assoul, M., Colas, G., Giampiccolo, S., Barbe, J.P. (2021). Finite element simulation and experimental investigation of the effect of clearance on the forming quality in the fine blanking process. *Microsystem Technologies*, vol. 27, p. 871-881, DOI:10.1007/s00542-020-04983-7.
- [21] Faura, F., Garcia, A., Estrems, M. (1998). Finite element analysis of optimum clearance in the blanking process. *Journal of Materials Processing Technology*, vol. 80-81, p. 121-125, DOI:10.1016/S09240136(98)00181-2.
- [22] Natpukkana, P., Pakinsee, S., Boonmapat, S., Mitsomwang, P., Borrisutthekul, R., Panuwannakorn, R., Khoa-phong, L. (2018). Investigation of notch shear cutting for JIS SCM420 steel wire rod. *IOP Conference Series: Materials Science and Engineering*, art. ID 012013, DOI:10.1088/1757-899X/436/1/012013.
- [23] Hambli, R., Richir, S., Crubleau, P., Tavel, B. (2003). Prediction of optimum clearance in sheet metal blanking processes. *The International Journal of Advanced Manufacturing Technology*, vol. 22, p. 20-25, DOI:10.1007/s00170-002-1437.
- [24] Engin, K.E., Eyercioglu, O. (2017). The effect of the thickness-to-die diameter ratio on the sheet metal blanking process. *Strojniški vestnik - Journal of Mechanical Engineering*, vol. 63, no. 9, p. 501-509, DOI:10.5545/sv-jme.2016.4272.
- [25] Engin, K.E., Eyercioglu, O. (2016). Investigation of the process parameters on the blanking of AISI 304 stainless steel by using finite element method. *Journal of Mechanics Engineering and Automation*, vol. 6, no. 7, p. 356-363, DOI:10.17265/2159-5275/2016.07.00-6.